FORMATION AND EVOLUTION OF NICKEL SILICIDES IN SILICON NANOWIRES

A. Katsman, M. Beregovsky, Y. E. Yaish

Technion
Haifa, Israel
akatsman@technion.ac.il

Accepted September 19, 2013

1. Introductıon

Quasi-one-dimensional semiconducting structures have been recently studied as potential candidates for electronic applications. Semiconducting nanowires (NW) have been implemented as the active channel of field effect transistor (FET) with linear and Schottky barrier source and drain contacts [1, 2]. SiNW FETs are of particular interest because they could allow the combination of one-dimensional transport and self-assembly techniques with the well-established Si technology. Of fundamental importance is the method in which contacts to the nanowire channel are being formed. Nickel silicide / silicon contacts used in FET can be formed by thermally activated axial intrusion of nickel silicides into the silicon NW (SiNW) from e-beam lithography pre-patterned Ni reservoirs located at both ends of the NWs. However, the formation of a precisely controlled nanostructure remains one of the most challenging problems in nanotechnology today.

Transformation of the longitudinal NW segments into single-crystalline nickel silicides throughout the entire NWs bulk has been interpreted by some investigators as evidence of a volume diffusion control process. However, the volume diffusion coefficients of nickel in Ni_2Si at 300 – 400 °C are inconsistent with observable nickel silicide intrusion lengths. The experimental results published so far show a distinct dependence of nickel silicide intrusion length on the silicon NW diameter [3], which is indicative of a surface diffusion or a surface reaction controlled process.

The kinetics of nickel silicide growth in Si NWs found by different authors [3 – 13] varies substantially, and the growth rates may differ by some orders of magnitude at the same temperature (for example, from ~ 0.01 nm / s at 500 °C [5] to ~ 4 nm / s at 450 °C [9] and ~ 5 nm / s at 420 °C [10]). Kinetic analysis of nickel silicide formation through point contact reaction between Si and Ni nanowires in the temperature range 500 – 650 °C was performed by Kuo-Chang Lu et al. [5]. A linear time dependence of the silicide length was found for all temperatures investigated, with growth rates of 0.01 – 0.1 nm / s [5]. Activation energies were obtained for the case of nickel diffusion through the silicon part of the NW (1.25 eV) and for diffusion through the nickel silicide phase (1.7 eV). The authors [5] proposed that the observed epitaxial growth of NiSi may be an interface reaction controlled process limited by the rate of dissolution of Ni into Si at the point contact interface and accompanied by very fast volume diffusion of interstitial nickel atoms. The kinetics of Ni silicide phase formation was studied by Dellas et al. [9] in the temperature range 400 – 550 °C for 50 – 75 nm-thick SiNWs grown in

<112> and <111> directions. For <112> oriented SiNWs, growth of the θ-Ni_2Si phase exhibited parabolic kinetics with activation energy of 1.45 ± 0.07 eV / atom. In the case of <111> oriented SiNW, the $NiSi_2$ was the only formed phase and the $NiSi_2$ growth demonstrated linear kinetics with activation energy of 0.76 ± 0.10 eV / atom [9]. Square root time dependence of the total silicide intrusion length was found by Ogata et al. [10] for different crystallographic orientations of SiNWs and core diameters ranging from ~ 10 to 100 nm. They found that the $NiSi_2$ was the first forming phase whereby Ni-rich silicide phases subsequently nucleate close to the Ni reservoir. Ogata et al. [10] also observed the retardation of silicide growth in oxidized SiNWs. A square root time dependence of the total intrusion length was found for nickel silicides formation in SiNWs at temperatures 350 – 440 °C [11]. Subsequent anneals of the samples at different temperature revealed Arrhenius-type temperature dependence of the square intrusion length increase with an activation energy of 1.45 ± 0.11 eV [11]. Transition from linear to parabolic growth of nickel silicides in SiNWs was analyzed by Yaish et al. [12]. The linear regime can be realized when transition of Ni atoms from the Ni reservoir towards the wire is hindered and limits the silicide growth, while the parabolic regime corresponds to fast transition of Ni atoms from the reservoir and the silicide growth is controlled by diffusion of Ni atoms along the silicide surface toward the silicon part. Intermediate regimes are realized in many cases [12]. Analysis of published experimental results [14] revealed that in many cases formation of nickel silicides in SiNWs can be controlled by diffusion of nickel along the silicide surface or silicide / SiO_2 interface.

The axial intrusion consists usually of different nickel silicides which grow simultaneously during thermal annealing. The kinetics of their growth inside the intrusion can be different with (or without) predominant growth of one of the silicides [15]. The growth is often accompanied by local thickening and tapering of the silicide NW [16 – 20], up to full disintegration of a NW segment adjacent to Si. Up to date, comprehensive understanding of these processes is still missing.

Simultaneous growth of different silicides in SiNWs during rapid thermal annealing (RTA) was recently analyzed in the framework of the model, taking into account the balance between transition of Ni atoms from the Ni reservoir to the NW surface, diffusion transport of these Ni atoms from the contact area to the interfaces between different silicides and nickel silicide / Si interface, and corresponding reactions of Ni atoms with Si and the nickel silicides formed [15]. Thickening and tapering of the silicide intrusion during repeated anneals can be explained by the presence of opposite atomic fluxes caused by curvature gradients. The latters are connected with the presence of two or more different nickel silicide phases along the intrusion segment [19, 20]. In order to understand what processes actually control the nickel silicide formation, corresponding activation energies should be found. For this purpose, time and temperature dependences of the silicide intrusion length should be properly measured.

In the present work we analyzed the experimental results on time and temperature dependencies and possible instability of two-phase nickel silicide intrusions in <110> and <112> oriented SiNWs for a temperature range of 300 – 440 °C and nanowire diameters of 30 – 60 nm obtained previously in our laboratory [11, 12, 19, 20]. The results were analyzed in the framework of diffusion model which was developed. This model includes the fluxes of Ni and Si atoms along the nickel silicides formed as well as the reactions at Si / silicide and silicide / silicide interfaces. Quantitative agreement between experiments and theory was obtained and discussed.

2. Experimental details

The SiNWs were synthesized by the vapor-liquid-solid growth technique in an ultrahigh vacuum chemical vapor deposition chamber, with silane as the silicon precursor and gold as the catalyst [21, 22]. Typical diameters of NWs grown in the <112> and <110> directions were 35 – 60 nm and 25 – 40 nm, respectively. SiNWs were oxidized at 700 °C by CVD reactor in oxygen flow with rate of 200 sccm and pressure of 1 atm. Samples were fabricated by a method described previously [11], with the lone exception being that the SiNWs were randomly dispensed from an ethanol suspension onto a sacrificial 150 nm-thick PMMA resist layer (deposited on the Si_3N_4 / Si substrate) which allowed to obtain a suspended SiNW structure. In order to form nickel silicide/silicon contacts, a series of anneals of the Ni/SiNW sample were performed: the first, at 420 °C for 15 s, followed by a few subsequent anneals, each at 440 °C for 5 s. Each anneal was carried out in a rapid thermal annealing (RTA) machine in a nitrogen atmosphere and included heating to (and cooling from) the annealing temperature with the rate of 1 °C / s. After every annealing, the silicide intrusions were investigated by high resolution scanning electron microscopy (HRSEM) and atomic force microscopy (AFM).

3. Main experimental results

The axial nickel silicide intrusions were formed as a result of a series of subsequent anneals at 420 and 440 °C. Simultaneous growth of two nickel silicides in SiNWs was observed in a number of works [11, 12, 15]. The typical results obtained in our laboratory are presented in **Figures 1 – 6**. Two-phase nickel silicide intrusions with different thickness of particular intrusion segments are shown in **Figure 1**. Time evolution of intrusion length in different SiNWs at 420 and 440 °C are presented in **Figure 2**. In order to estimate effective activation energy of the process, a number of samples were annealed for 30 s subsequently at 300, 350, 400, 420 and 440 °C. One of such samples is shown in **Figure 3**.

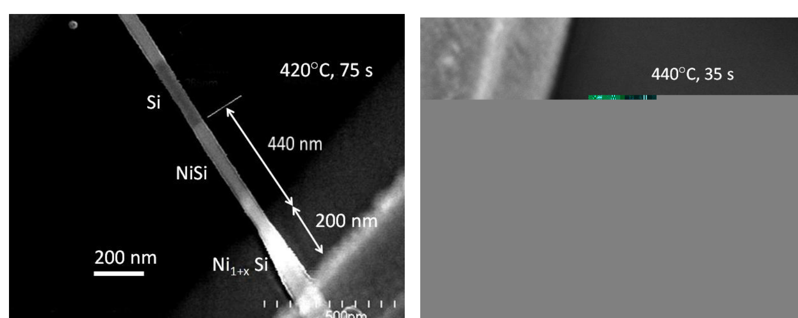

Figure 1. Two-phase nickel silicide intrusions in SiNWs after different rapid TA.

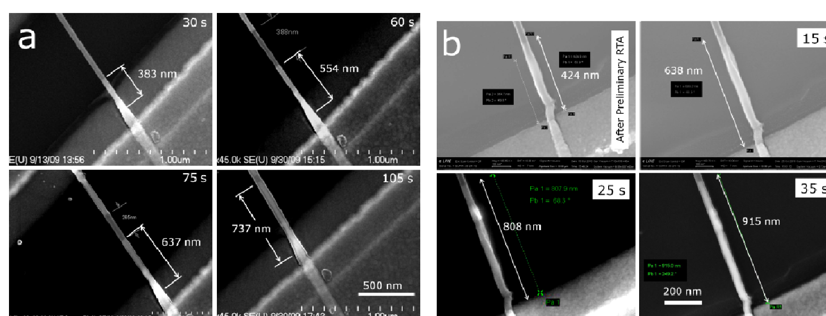

Figure 2. HRSEM micrographs of SiNWs with Ni-silicide intrusions formed during rapid thermal annealing (RTA) for different times at 420 (a) and 440 °C (b).

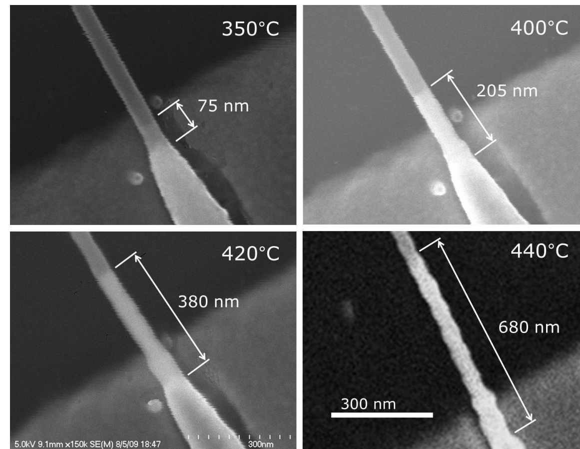

Figure 3. HRSEM images of SiNW covered by 140 nm Ni / 2 nm Au after subsequent RT anneals at 350, 400, 420, and 440 °C for 30 s each; the SiNW has the core diameter of 30 nm and native oxide shell of 3 nm.

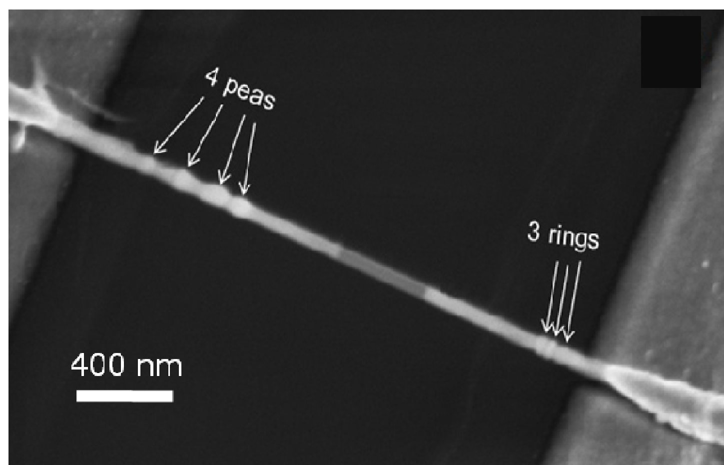

Figure 4. HRSEM images of a 28 nm-thick Ni / SiNW structure after five subsequent thermal cycles with annealing temperatures of 420 °C for 15 s (two first) and 440 °C for 5 s (three last).

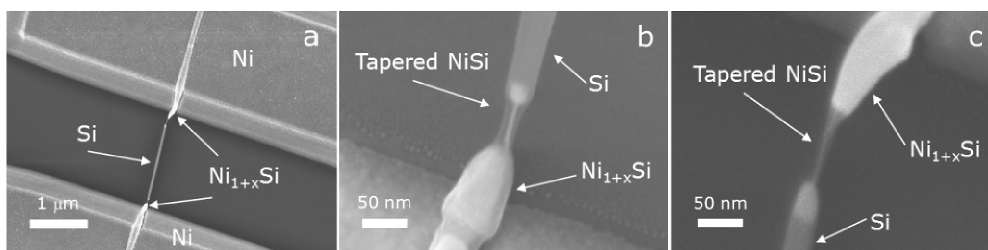

Figure 5. HRSEM image of Ni / SiNW structure after thermal annealing at 420 °C for 1 s: (a) total view of the NW structure with two tapered NiSi regions; (b) and (c) bottom and upper parts of the NW structure.

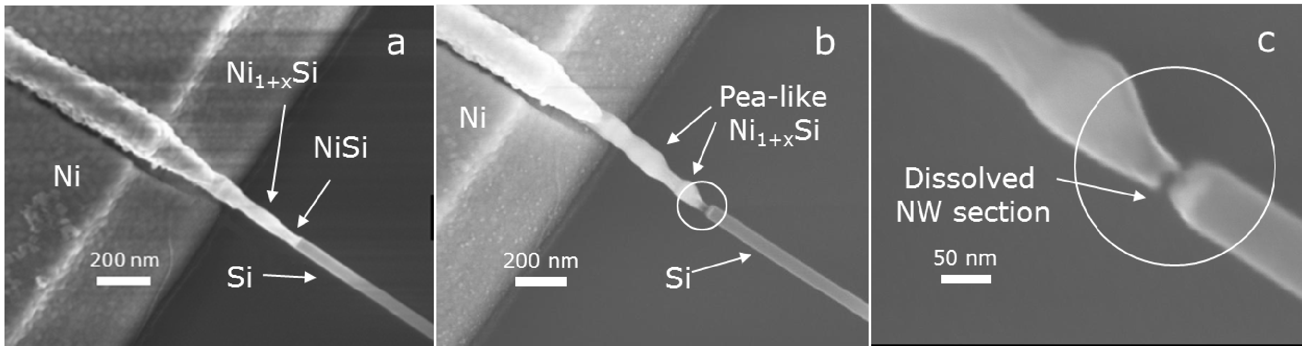

Figure 6. HRSEM images of the a 52 nm-thick Ni / SiNW structure as a result of TA at 420 °C for 15 s (a), followed by two subsequent anneals each at 440 °C or 5 s (b); (c) magnification of the dissolved NW section in (b). (The NW integrity is apparently kept here by a 5 nm-thick thermal oxide shell).

The morphological peculiarities of the silicide intrusions observed sometimes as alternate thickening (pea- and ring-like structures, **Figure 4**), and tapering of the NW segments (**Figure 5**). In some instances the NW tapering continued up to full dissolution / disintegration of the silicide segment adjacent to the Si NW (**Figures 6b** and **c**).

4. Theoretıcal model

Simultaneous growth of several nickel silicides in Si nanowires (SiNWs) is controlled by some sequential processes: (a) transition of Ni atoms from the e-gun deposited Ni reservoir through an intermediate contact layer (formed by Si oxides or another contamination of the Si surface before Ni deposition) to the silicon or the nickel silicide surface; (b) diffusion transport of these Ni atoms from the contact area to the reaction interfaces; (c) reaction of Ni atoms with Si or nickel silicides at the reaction interfaces resulting in the growth of different nickel silicides (**Figure 7**).

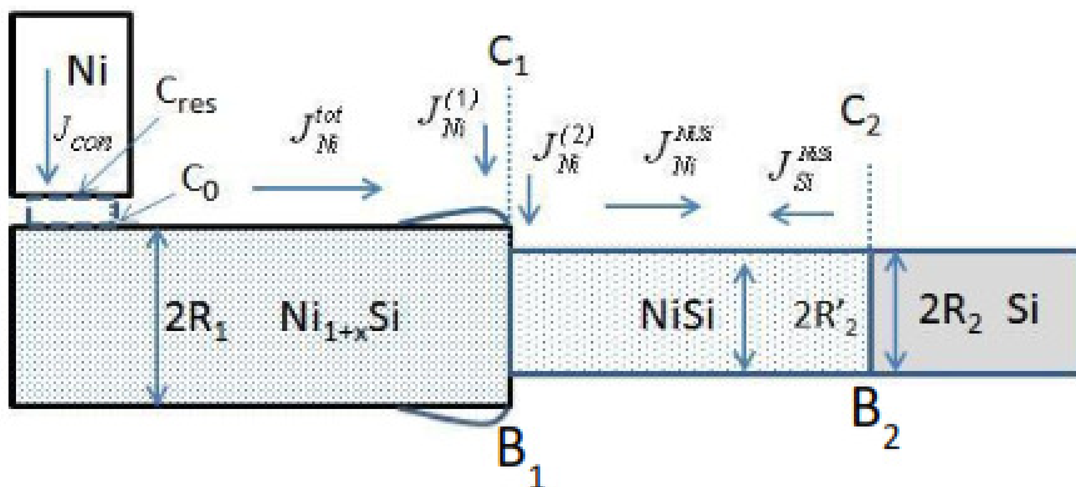

Figure 7. Evolution of nickel silicide intrusion during RTA, schematic diagram.

Experimentally observed thickening and thinning of different parts of the nickel silicide intrusion, up to full dissolution of some part of the intrusion, cannot occur without some diffusion of silicon atoms. In the model considered below, the Si atoms diffuse along the NiSi surface, reach the boundary NiSi / $Ni_{1+x}Si$ ($x > 0$) and react there with the Ni atoms arriving this boundary from the Ni source to form a new portion of $Ni_{1+x}Si$ phase (**Figure 7**). Without loss of generality, we use $x = 1$ in the following discussion.

The flux of Ni atoms from the reservoir through the contact layer of thickness h is proportional to the contact area, s_{con}:

$$J_{con} = -\Lambda_{tr} \frac{\mu_{res} - \mu_0}{h} s_{con}, \quad (1)$$

where Λ_{tr} is the kinetic coefficient for transition of Ni from the reservoir to the silicide surface, μ_{res} and μ_0 are the Ni chemical potentials in the Ni reservoir and on the intrusion surface near the Ni source, respectively. This flux is equal to the total flux of nickel atoms, J_{Ni}^{tot}, diffusing then along the nickel-rich silicide surface:

$$J_{Ni}^{tot} = J_{con}. \quad (2)$$

The total flux of nickel atoms arriving the Ni_2Si / NiSi boundary (B_1) can be divided into three parts:

$$J_{Ni}^{tot} = J_{Ni}^{NiSi} + J_{Ni}^{(1)} + J_{Ni}^{(2)}, \quad (3)$$

where $J_{Ni}^{(1)}$ and $J_{Ni}^{(2)}$ are the fluxes of Ni atoms reacting with Si atoms arriving this boundary and with NiSi phase, respectively. J_{Ni}^{NiSi} is the flux of nickel atoms that diffuse along NiSi surface and reach the NiSi / Si boundary (B_2). The corresponding reactions at boundary B_1 can be written as follows:

$$2\,Ni + Si \rightarrow Ni_2Si \quad (B_1) \quad (4)$$

$$Ni + NiSi \rightarrow Ni_2Si \quad (B_1) \quad (5)$$

$$Ni + Si \rightarrow NiSi \quad (B_2) \quad (6)$$

The reaction (4) is provided by supply of Si atoms along the NiSi surface by the flux J_{Ni}^{NiSi}. Assuming $J_{Ni}^{NiSi} = \theta J_{Ni}^{NiSi}$ and $J_{Ni}^{(1)} = 2 J_{Si}^{NiSi}$, Eq. (3) can be rewritten:

$$J_{Ni}^{tot} = J_{Ni}^{NiSi}(1 + 2\theta) + J_{Ni}^{(2)}. \quad (7)$$

In a steady state condition, diffusion fluxes of Ni atoms are the following:

$$J_{Ni}^{tot} = \Lambda_1 \frac{\mu_0 - \mu_1}{L_1} s_1, \quad (8)$$

$$J_{Ni}^{NiSi} = \Lambda_2 \frac{\mu_1 - \mu_2}{L_1} s_2, \quad (9)$$

where Λ_1 and Λ_2 are the kinetic coefficients along the Ni_2Si and NiSi segments of intrusion, L_1 and L_2 are the lengths of Ni_2Si and NiSi segments, μ_1 and μ_2 are the Ni chemical potentials at the Ni_2Si / NiSi boundary (B_1), and at the NiSi / Si boundary (B_2), respectively. $s_1 = 2\pi R_1 \delta$, and $s_2 = 2\pi R_2 \delta$, where δ is the diffusion surface layer thickness. The reaction flux $J_{Ni}^{(2)}$ can be written by analogy to the fluxes (8) and (9):

$$J_{Ni}^{(2)} = \Lambda_{reac} \frac{\mu_1 - \mu_{reac}}{R_1} s_{reac}, \quad (10)$$

where L_{reac} is the kinetic coefficient of reaction (5) and μ_{reac} is the chemical potential of Ni atoms at the NiSi / Ni_2Si interface (B_1) after reaction.

Using Eqs. (1, 7 – 10) one can find the values of μ0 and μ1 as functions of μ_{res}, μ_{reac}, μ_2 and of dimensionless intrusion lengths $l_1 = L_1 / R_1$ and $l_2 = L_2 / R_1$:

$$\mu_0 = \frac{l_1\mu_{res} + q_0\mu_1}{l_1 + q_0}, \tag{11}$$

$$\mu_1 = \frac{f_0 l_2 \mu_{res} + (q_0 + l_1)(\mu_2 + p_0 l_2 \mu_{reac})}{f_0 l_2 + (q_0 + l_1)(p_0 l_2 + 1)}, \tag{12}$$

where $f_0 = L_1 s_1 / L_2 s_2 (1+2\theta)$, $q_0 = L_1 s_1 h / L_{tr} s_{con} R_1$, and $p_0 = L_{reac} s_{reac} / L_2 s_2$. When the fluxes of nickel, described by Eqs. (8) and (9), are directed from the Ni reservoir to the silicon part of the NW ("positive" direction), the silicide intrusions, l_1 and l_2, grow with different kinetics, from linear to parabolic, depending on kinetic, geometric and contact parameters.

The nickel-rich silicide grows due to reactions (4) and (5) at a rate proportional to corresponding fluxes:

$$\frac{dL_1}{dt} = \frac{(2+x)\Omega_1}{x\pi R_1^3}(J_{Ni}^{(2)} + xJ_{Si}^{NiSi}) = \frac{3\Omega_1}{\pi R_1^2}(J_{Ni}^{(2)} + \theta J_{Ni}^{NiSi}). \tag{13}$$

The monosilicide grows at the NiSi / Si interface due to reaction (6) and it is contracted due to reaction (5) at the intersilicide interface:

$$\frac{dL_2}{dt} = \frac{2\Omega_2}{\pi R_2^3} J_{Ni}^{NiSi} - \frac{(2+x)\Omega_2}{x\pi R_2^2} J_{Ni}^{(2)}. \tag{14}$$

In the dimensionless form it can be rewritten as follows:

$$\frac{dl_1}{d\tau} = \frac{6\delta}{R_1(1+2\theta)} \frac{((\bar{\mu}_{res} - \bar{\mu}_{reac}) l_2 p_0 + (\bar{\mu}_{res} - \bar{\mu}_2)\theta) - p_0(q_0 + l_1)(\bar{\mu}_{reac} - \bar{\mu}_2)(1-\theta)/f_0}{l_2 f_0 + (q_0 + l_1)(p_0 l_2 + 1)}, \tag{15}$$

$$\frac{dl_2}{d\tau} = -\frac{4R_1\delta\nu}{R_2^2(1+\theta)} \frac{(\bar{\mu}_{res} - \bar{\mu}_2) + (\bar{\mu}_{reac} - \bar{\mu}_2)(q_0 + l_1) p_0 / f_0}{l_2 f_0 + (q_0 + l_1)(p_0 l_2 + 1)} - \frac{2R_1^2\nu}{(2+x)R_2^2}\frac{dl_1}{d\tau}, \tag{16}$$

where $\tau = \Lambda_1\Omega_1 kTt / R_1^2$, $\nu = \Omega_2 / \Omega_1$, and $\bar{\mu}_i \equiv \mu_i / kT$.

It should be noted that for zero initial values $l_1^0 = 0$ and $l_2^0 = 0$, a solution of the equation system (15) and(16) satisfying the following initial conditions has to be found:

$$l_1 = 0, \qquad l_2 \le \bar{l}_2 \equiv \frac{q_0(\mu_{reac} - \mu_2)(1-\theta) - (\mu_{res} - \mu_2)\theta f_0 / p_0}{f_0(\mu_{res} - \mu_{reac})}, \tag{17a}$$

$$l_2 = 0, \qquad t = 0, \tag{17b}$$

The first condition corresponds to the requirement $\mu_1 > \mu_{reac} - \theta(\mu_1 - \mu_2) / p_0 l_2$ providing the growth of the nickel-rich silicide. It means, that the monosilicide starts to grow first, and the nickel-rich silicide starts to grow only when the length of the monosilicide reaches a critical value $\bar{l}_2$. If $\theta = 0$, the requirement (17a) simply provides reaction (5) as has been found in [14].

Introducing the contact "window": $\bar{w} \equiv s_{con}\delta / s_1 h$ and dimensionless parameters $r_1 = R_1 / \delta$, $r_2 = R_2 / \delta$, $d_{12} = L_2 / L_1$, $d_{1tr} = L_{tr} / L_1$, and $d_{1reac} = L_{reac} / L_1$, one can write $f_0 \equiv r_1 / (1+\theta) r_2 d_{12}$, $q_0 \equiv 1 / r_1 d_{1tr} \bar{w}$, and $p_0 \equiv r_1 d_{1reac} \bar{w} / r_2 d_{12}$.

The system of Eqs. (13) and (14) was solved numerically for different parameters μ_{res}, μ_{reac}, μ_2, θ, r_1, r_2, ν, d_{12}, d_{1tr} and d_{1reac}. Typical solutions shown in **Figure 8** demonstrate possible dominant growth of one of two phases.

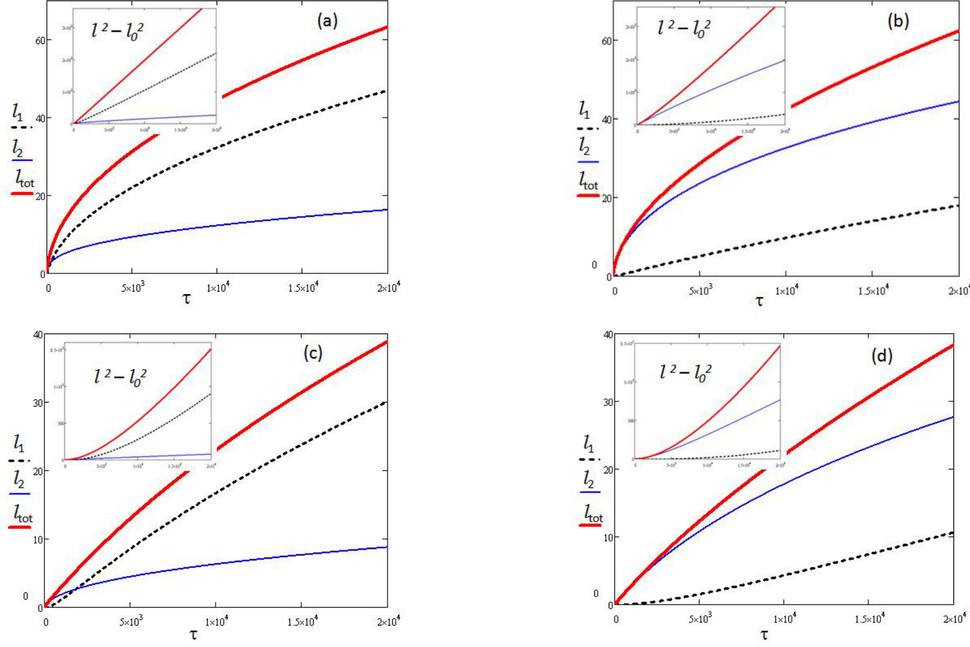

Figure 8. Calculated dimensionless nickel silicide lengths for different kinetic and geometrical parameters: (a, b) – square root like and (c, d) linear-like dependencies with dominant growth of mono- (b, d) or Ni-rich silicide (a, c).

In two limiting cases: (1) $L_2 = 0$ and (2) $L_{reac} = 0$, $\theta = 0$ – only one silicide phase grows (Ni-rich or NiSi, respectively). In these cases the system of Eqs. (13) and (14) is reduced to one equation

$$\frac{dl_i}{d\tau} = \frac{n_i}{r} \frac{\bar{\mu}_{res} - \bar{\mu}_2}{l_i + q_i} \tag{18}$$

with the following solution:

$$l_i = \sqrt{\alpha_i \tau + (l_0 + q_i)^2} - q_i , \tag{19}$$

where $\alpha_i = 2(\bar{\mu}_{res} - \bar{\mu}_2) n_i / r_i$ and $q_i = \Lambda_i / \Lambda_{tr} r_i \bar{w}$, $i = 1$ or 2 for the two limiting cases mentioned above. Eq. (18) is similar to the relationship obtained earlier for the case of one nickel silicide growth [8]. The dependence $l_i(\tau)$, Eq. (18), is linear-like for experimental times:

$$\tau << \tau_{crit} \equiv (l_0 + q_i)^2 / \alpha_i . \tag{20}$$

Such a case may be realized for sufficiently small contact "windows", $\bar{w}$, and can be referred to as "contact" growth regime. In the opposite case, $\tau >> \tau_{crit}$, the dependence $l_i(\tau)$ is square root-like, and the silicide growth is diffusion controlled.

5. Analysıs of experımental results

The silicide intrusions were obtained by annealing of SiNWs for different temperatures and times as described in [12]. Examples of linear and square root-like time dependences observed for the Ni-rich part and NiSi part of intrusions at 420 and 440 °C are presented in **Figure 9**.

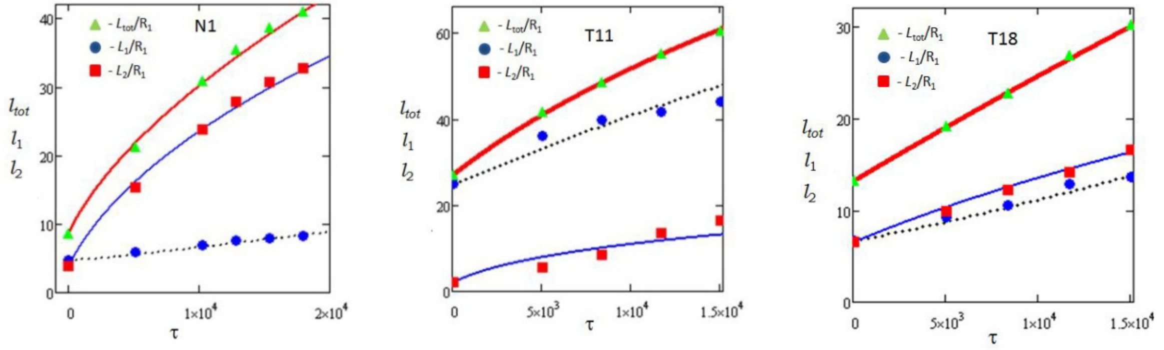

Figure 9. Typical kinetics of total and particular silicide intrusion lengths; dots are experimental values [12], solid lines are calculated with parameters given in **Table 1**.

Table 1. Fitting parameters used in the calculation of particular silicide intrusion lengths.

	T, °C	l_{01}	l_{02}	$\overline{w}$, 10^{-3}	d_{21}	d_{1reac}	d_{1tr}	r_1	r_2	$\overline{C}$
N1	420	4.7	3.9	3.03	1	0.01	1	36	30	0.56
T11	440	25.6	2.1	10	2.7	0.7	1	36	30	0.51
T18	440	6.7	6.5	0.43	2.7	0.2	1	36	30	0.50

The experimental results are well described by Eqs. (15, 16) with the corresponding parameters mentioned in **Table 1**. It should be noted that preliminary heating of SiNWs to 400 °C, exposure at this temperature followed by slow heating to 420 or 440 °C resulted in preliminary formation of both Ni-rich and NiSi parts; their lengths are used in the present calculation as initial lengths l_{01} and l_{02}.

Substantial growth of NiSi at 420°C and 440°C as compared to the dominant growth of Ni-rich silicides at lower temperatures (usually $l_{01} > l_{02}$) is indicative of relatively lower rates of reactions (4) and (5) at higher temperatures. Surface diffusion coefficients along Ni-rich silicide can be evaluated as $5 \cdot 10^{-14}\ m^2/s$ at 420 °C and $1 \cdot 10^{-13}\ m^2/s$ at 440 °C. The diffusion coefficient along the monosilicide surface is of the same order at 420 °C ($d_{21} = 1$), but of about 3 times higher at 440 °C ($d_{21} = 2.7$). For sample N1, the critical time, $\tau_{crit} = 1.5 \cdot 10^3$, Eq. (20), the growth occurs mainly at $\tau > \tau_{crit}$, and the time dependence of the total intrusion length is square root-like; the same is true for the NiSi part, but the Ni-rich silicide part grows almost linearly, due to a low reaction rate, d_{r1}. For sample T11, the "window" value, $\overline{w} = 0.1$, is sufficiently high, $\tau_{crit} = 140$, and the growth occurs in the diffusion controlled regime for both parts of the intrusion. For sample T18, the contact "window" is small, $\overline{w} = 4.3 \cdot 10^{-4}$, the experimental times $\tau < \tau_{crit} = 7.3 \cdot 10^4$, and both parts of the intrusion increase linearly with time; in this case the total growth rate is determined by the transfer of Ni atoms from the reservoir, and the particular rates depend on the reaction rate, d_{1tr}, at the $Ni_{1+x}Si$ / NiSi interface. In general case, square root time dependence can be realized for the total silicide length (in the diffusion controlled regime), while particular silicides may have different kinetics (square root, linear or intermediate) depending on the reaction rate of the silicide transformations. In this case, assuming close values of diffusion coefficients of Ni along different silicide / SiO_2 interfaces, or, at least, their close activation energies, the total silicide length can be well described by the simplified dependence

$$L^2 - L_0^2 = 8D_s\Delta t(C_{res} - C_f)\frac{\delta}{R} \equiv A_0^2 \exp\left(-\frac{E}{kT}\right)\Delta t \equiv A^2(T)\Delta t\,. \tag{21}$$

Analysis of temperature dependence of the square length increase, ΔL_n^2, after RTAs at subsequent temperatures, T_n and T_{n+1}, each for 30 s, allows evaluating the activation energy of the process by using L_{T_n} as the initial length, $L_{0,T_{n+1}}$, for the subsequent anneal at temperature T_{n+1}:

$$\Delta L_n^2 \equiv L_{T_{n+1}}^2 - L_{0,T_{n+1}}^2 \approx L_{T_{n+1}}^2 - L_{T_n}^2 = A^2(T_{n+1})\Delta t\,, \tag{22}$$

Such analysis should take into account the silicide growth during heating to and cooling from the annealing temperature. The increase of the silicide intrusion length during heating / cooling with the rate α from T_0 to T_{n+1}, can be evaluated with the following expression:

$$L_{0,T_{n+1}}^2 - L_{T_n}^2 = A_0^2\int_0^{\Delta t}\exp\left(-\frac{E}{k(T_0+\alpha t)}\right)dt = A^2(T_0)\int_0^{\Delta t}\exp\left(\frac{E\alpha t}{kT_0(1+\alpha t)}\right)dt \approx$$
$$\approx A^2(T_0)\frac{kT_0^2}{E\alpha}\left(\exp\left(\frac{E\alpha\Delta t}{kT_0^2}\right) - 1 - \frac{1}{2}\sqrt{\frac{\pi E}{kT_0}}erf\left(\frac{\alpha\Delta t}{T_0}\sqrt{\frac{E}{kT_0}}\right)\right), \tag{23}$$

where $\Delta t = (T_{n+1} - T_0)/\alpha$ is the heating time. The activation energy of the diffusion process, E, can be found by the iteration procedure described in detail in [9]. The activation energy averaged over the examined NWs is $E = 1.45 \pm 0.11$ eV. This activation energy is typical for nickel silicide growth in thin film silicide reactions controlled by interface and grain boundary diffusion processes [23 – 26].

5.1. Possible instabilities of two-phase nickel silicide intrusions

The sign of the flux J_{Ni}^{NiSi}, Eq. (9), is determined by the difference of the chemical potentials:

$$\mu_1 - \mu_2 = \frac{f_0(\mu_{res} - \mu_2) + p_0(q_0 + l_1)(\mu_{reac} - \mu_2)}{f_0 + (q_0 + l_1)(p_0 + 1/l_2)}\,. \tag{24}$$

As stated before, the chemical potentials μ_{res}, μ_{reac}, and μ_2 depend on the surface curvature [18]:

$$\mu_{res} = \mu_{res0} + \gamma\Omega/R_1\,, \qquad \mu_{reac} = \mu_{reac0} + \gamma\Omega/R_1\,, \qquad \mu_{2s} = \mu_{20} + \gamma\Omega/R_2\,, \tag{25}$$

where γ is the surface energy. If $\mu_{reac} < \mu_2$ (can be possible due to the curvature term), the difference $\mu_1 - \mu_2$ decreases with increasing of the nickel-rich silicide length, l_1, and reaches zero at a critical value:

$$l_1^{crit} = \frac{f_0}{p_0}\frac{\mu_{res0} - \mu_{20} - \gamma\Omega\Delta R/R_1R_2}{\mu_{20} - \mu_{reac0} + \gamma\Omega\Delta R/R_1R_2} - q_0\,. \tag{26}$$

For values $l_1 > l_1^{crit}$, the flux J_{Ni}^{NiSi} reverses its direction, and the nickel atoms are transferred from the NiSi to the Ni-rich part of intrusion. The critical value l_1^{crit} can be estimated assuming $f_0 = 1$, $\mu_{res0} - \mu_{20} \approx kT >> \gamma\Omega\Delta R/R_1R_2$ and $|\mu_{20} - \mu_{reac}| << \gamma\Omega\Delta R/R_1R_2$ and using typical values $\gamma = 2$ J / m², $\Omega = 1.2 \cdot 10^{-29}$ m³, $kT = 9.29 \cdot 10^{-21}$ J, $R_1 = 12$ nm, $R_2 = 10$ nm:

$$l_1^{crit} \approx \frac{kTR_1R_2}{p_0\gamma\Omega\Delta R} - q_0 \approx \frac{30}{p_0} - q_0\,. \tag{26a}$$

This length can vary over a wide range of values depending on parameters of reaction (5) (incorporated in parameter p_0) and on supply of Ni atoms from reservoir (parameter q_0). For example, for $p_0 = q_0 = 1$, $l_1^{crit} = 29$. It should be noted that the flux J_{Ni}^{tot} does not change its direction since the difference of chemical potentials, $\mu_0 - \mu_1$, remains positive for all values of l_1:

$$\mu_0 - \mu_1 = \frac{\mu_{res} - \mu_2 + p_0 l_2 (\mu_{res} - \mu_{reac})}{f_0 l_2 / l_1 + (1 + q_0 / l_1)(p_0 l_2 + 1)}. \tag{27}$$

5.2. Local thickening: formation of rings and pea-like bulges

As it was found, first anneals resulted in formation of two-phase silicide intrusion consisted of two segments with different radii (**Figures 1a**, **b**, and **3a**). Repeated anneals are often resulted in local thickening of the intrusion with formation of periodic rings and pea-like bulges. Annealing at comparatively low temperatures (during heating and cooling in the temperature range 350 – 400 °C) may cause evolution of the intrusion in the Ni_2Si / NiSi boundary region: the critical length, l_1^{crit}, decreases with temperature (mainly, due to increase of $p_0 \sim L_{reac} / L_2$, Eq. (23)). As a result, the length l_1, achieved in a previous annealing may exceed the critical value, l_1^{crit}, Then, the flux of Ni atoms along the NiSi part of intrusion reverses its direction, and the net flux of atoms along the NiSi part becomes negative, since the flux of Si atoms is always directed from Si towards the nickel pad. It provides dissolution of the NiSi phase and thinning of its segment adjacent to the Ni_2Si and thickening of the latter. The result of such process can be seen, for example, in **Figure 3a**. The Ni atoms diffusing from the Ni pad reach the Ni_2Si / NiSi boundary region and accumulate here, in the region of the minimal chemical potential, μ_1. In order to evaluate possible thickening of the Ni_2Si / NiSi boundary region, one can estimate the number of additional Ni atoms reaching this region for the case $f_0 = p_0 = q_0 = 1$ and l_1, $l_2 >> 1$:

$$\frac{\Delta N}{\Delta t} = \Lambda_1 \frac{\mu_0 - \mu_1}{L_1} s_1 + \Lambda_2 \frac{\mu_2 - \mu_1}{L_2} s_1 \approx \Lambda_1 \frac{\mu_{res} - \mu_{reac}}{L_1} s_1 + \Lambda_2 \frac{\mu_2 - \mu_{reac}}{L_2} \frac{\Delta l}{l_1} s_1, \tag{28}$$

where $\Delta l = l_1 - l_1^{crit}$. Using the following expressions for kinetic coefficients: $\Lambda_1 = D_i \bar{c}_i / kT\Omega$, where D_i and $\bar{c}_i$ are the surface diffusion coefficient and average Ni concentration on segment i of intrusion ($i = 1, 2$) and Eqs. (25), one can obtain:

$$\frac{\Delta N}{\Delta t} = 2\pi \frac{\delta}{\Omega} \left(D_1 \frac{c_0 - c_1}{l_1} + D_2 \frac{\gamma\Omega}{kT} \frac{c_2}{l_2} \frac{\Delta R}{R_1^2} \right). \tag{28a}$$

Assuming thickening in the shape of torus with the tube radius Δr, additional volume can be written as $\Delta V = \Delta N \Omega = \pi^2 R_1 (\Delta r)^2$. The thickening Δr can be estimated as

$$\Delta r = \sqrt{\frac{2\delta}{\pi R_1} D_1 \Delta t \frac{\Delta c}{l_1} \left(1 + \frac{D_2}{D_1} \frac{\gamma\Omega}{kT} \frac{\bar{l}_1 \bar{c}_2}{l_2 \Delta c} \frac{\Delta R}{R_1^2} \right)}, \tag{29}$$

For $D_1 = D_2 = 4 \cdot 10^{-15}$ m²/s, $\Delta t = 30$ s, $\delta = 0.5$ nm, $l_1 = 40$, $l_2 = 10$, $R_1 = 15$ nm, $\Delta R = 2$ nm, and $\gamma\Omega / kT = 2.6$ nm, one can obtain $\Delta r \approx 5$ nm, that is close to real size of pea-like bulges.

Next annealing at higher temperature (when l_1, turns out to be less than the critical value, l_1^{crit}), providing supply of nickel atoms from the Ni pad causes further growth of both parts of the silicide intrusion.

5.3. Tapering and dissolution of the NiSi segment

Thickening and formation of rings and bulges in the Ni_2Si / NiSi boundary region during repeated anneals may cause substantial decrease of the critical length l_1^{crit} due to local increase of ΔR (see Eq. (23a)). By this way the condition $l_1 > l_1^{crit}$ can be met at higher temperature, and the flux of Ni atoms along the NiSi part of intrusion reverses its direction. In this case the flux cannot be longer constant along the NiSi intrusion. At the Si / NiSi interface the flux of Ni atoms should be equal zero (there is no a source of Ni atoms here). Maximum atomic flux from the NiSi to the Ni_2Si will be realized at the NiSi / Ni_2Si interface where the gradient curvature is maximal. For $l_1 \geq l_1^{crit}$ the difference of chemical potentials, Eq. (9), can be approximated as follows:

$$\mu_1 - \mu_2 = \frac{\Delta l_1 p_0 (\mu_{reac} - \mu_2)}{f_0 + (q_0 + l_1)(p_0 + 1/l_2)} \approx -\frac{\Delta l_1}{l_1} \frac{\gamma \Omega \Delta R}{R_1 R_2}. \tag{30}$$

The corresponding Ni flux determines the rate of dissolution of the NiSi part of intrusion. It should be emphasized that dissolution of NiSi phase requires both Ni and Si fluxes being equal in their value and direction. Then, the total atomic flux along the NiSi intrusion, $J_{tot}^{NiSi} = 2J_{Ni}^{NiSi}$. Assuming a linear increase of J_{tot}^{NiSi} from zero to $2J_{Ni}^{m}$, the rate of dissolution can be written as:

$$\frac{dR_2}{dt} = \Omega \delta \frac{\partial J_{tot}^{NiSi}}{\partial x} = \Omega \delta \frac{2J_{Ni}^{m}}{L_2} = -D_2 C_1 \frac{\Delta l_1}{l_1 l_2} \frac{\gamma \Omega \delta (R_1 - R_2)}{kTR_1^3 R_2}. \tag{31}$$

Furthermore, let R_1 and l_2 be constant, and $l_1 = l_1^{crit} + \alpha\sqrt{t}$, where $\alpha = (2/R_1)\sqrt{D_1 \delta / R_1}$ [8], then integration of Eq. (28) results in the following equation:

$$R_1 \ln \frac{R_1 - R_2}{R_1 - R_2^0} - R_2^0 + R_2 = B\left(t - \frac{2l_{crit}\sqrt{t}}{\alpha} + \frac{2l_{crit}^2}{\alpha^2} \ln\left(1 + \frac{\alpha\sqrt{t}}{l_{crit}}\right)\right), \tag{32}$$

where $B = D_2 C_1 \gamma \Omega \delta / kTR_1^3 l_2$. The time of full dissolution (when $R_2 = 0$) can be found from Eq. (32). For the case $\alpha\sqrt{t} << l_1^{crit}$ it can be estimated by the expression:

$$t_{dis} \approx \left(\frac{3l_{crit}}{2\alpha B} \left(R_1 \ln \frac{R_1}{R_1 - R_2^0} - R_2^0 \right)\right)^{2/3}. \tag{33}$$

For $D_1 = D_2 = 2 \cdot 10^{-14}$ m^2 / s, $R_1 = 15$ nm, $R_2^0 = 13$ nm, $\delta = 0.5$ nm, $\alpha = (2/R_1)\sqrt{D_1 \delta / R_1} = 5.4$ s$^{-1/2}$, $l_{crit} = 30$, $C_1 = 0.67$, $\gamma\Omega = 2nm$, $l_2 = 10$ one can obtain $B \approx 1.0$ nm / s and $t_{dis} \approx 70$ s. Such values of dissolution time were often observed in the experiments.

6. Conclusıon

Evolution of nickel silicide intrusions in the NiSi / Si NWs after a series of rapid thermal anneals at different temperatures of 350 – 440 °C was analyzed in the framework of the phenomenological model taking into account the balance between transition of Ni atoms from

the Ni reservoir to the NW surface, diffusion transport of these Ni atoms and corresponding Ni/Si and Ni/nickel silicide reactions. Simultaneous formation of different nickel silicide phases during RTA was considered. Linear or square root-like growth kinetics of particular silicides and of total silicide intrusion length can be realized depending on both the "contact window" value and the relative rate of Ni-rich silicide formation. A square root time dependence of the total intrusion length was indicating of diffusion controlled process. The NW curvature gradients appearing due to different radii of different silicides may play substantial role in tapering and dissolution of monosilicide segment of intrusion. Subsequent anneals of the samples at different temperature revealed Arrhenius-type temperature dependence of the square intrusion length increase with an activation energy of 1.45 ± 0.11 eV typical for diffusion of Ni along the nickel silicide surface or nickel silicide / SiO_2 interface. Thermal cycling resulted in sequential thickening of nickel-rich part with formation of rings or pea-like bulges at different sides of the same NW. It was accompanied by tapering of the monosilicide part up to its full dissolution and breaking of the NW. For a certain set of model parameters formation of the pea-like profile on the nickel-rich silicide surface, tapering and dissolution of the monosilicide part of intrusion were obtained.

References

1. Y. Cui, Z. Zhong, D. Wang, W. U. Wang, C. M. Lieber. Nano Lett. 3 (2003) 149.
2. M. Mongillo, P. Spathis, G. Katsaros, P. Gentile, S. de Franceschi. Nano Lett. 12 (2012) 3074.
3. J. Appenzeller, J. Knoch, E. Tutuc, M. Reuter, S. Guha. In: Int. Electron Devices Meeting (2006).
4. W. M. Weber, L. Geelhaar, A. P. Graham, E. Unger, G. S. Duesberg, M. Liebau, W. Pamler, C. Chze, H. Riechert, P. Lugli, F. Kreupl, Nano Lett. 6 (2006) 2660.
5. K.-Ch. Lu, W.-W. Wu, H.-W. Wu, C. M. Tanner, J. P. Chang, L. J. Chen, K. N. Tu. Nano Lett. 7 (2007) 2389.
6. Y. Hu, J. Xiang, G. Liang, H. Yan, C. M. Lieber. Nano Lett. 8 (2008) 925.
7. W. M. Weber, L. Geelhaar, E. Unger, C. Chèze, F. Kreupl, H. Riechert, P. Lugli, Phys. Status Solidi B 244 (2007) 4170.
8. N. S. Dellas, B. Z. Liu, S. M. Eichfeld, C. M. Eichfeld, T. S. Mayer, S. E. Mohney. J. Appl. Phys. 105 (2009) 094309.
9. N. S. Dellas, M. Abraham, S. Minassian, C. Kendrick, S. E. Mohney. J. Mater. Res. 26 (2011) 2282.
10. K. Ogata, E. Sutter, X. Zhu, S. Hofmann. Nanotechnol. 22 (2011) 365305.
11. M. Beregovsky, A. Katsman, E. M. Hajaj, Y. E. Yaish, S. S. Elect. 80 (2013) 110.
12. Y. E. Yaish, A. Katsman, G. M. Cohen, M. Beregovsky. J. Appl. Phys. 109 (2011) 094303.
13. S. Habicht, Q. T. Zhao, S. F. Feste, L. Knoll, S. Trellenkamp, B. Ghyselen, S. Mantl. Nanotechnol. 21 (2010) 105701.
14. A. Katsman, Y. Yaish, E. Rabkin, M. Beregovsky. J. Elect. Mater. 39 (2010) 365.
15. A. Katsman, Y. Yaish, M. Beregovsky. Def. & Diff. Forum 323-325 (2012) 427.
16. Y.-Ch. Lin, Y. Chen, D. Xu, Y. Huang. Nano Lett. 10 (2010) 4721.
17. W. Tang, S. A. Dayeh, S. T. Picraux, J. Y. Huang, K. Tu. Nano Lett. 12 (2012) 3979.

18. Y. Chen, Y. C. Lin, C. W. Huang, C. W. Wang, L. J. Chen, W. W. Wu, Y. Huang, Nano Lett. 12 (2012) 3115.
19. A. Katsman, M. Beregovsky,Y. Yaish. In: MRS Proc. 1408 (2012) 93.
20. A. Katsman, M. Beregovsky, Y. Yaish. J. Appl. Phys.113 (2013) 084305.
21. J. Westwater, D. P. Gosain, S. Tomiya, S. Usui, H. Ruda. J. Vac. Sci. & Technol. B 15 (1997) 554.
22. A. M. Morales, C. M. Lieber. Science 279 (1998) 208.
23. J. W. Mayer, J. M. Poate, K. N. Tu. Science 190 (1975) 228.
24. J. O. Olowolafe, M. A. Nicolet, J. W. Mayer. Thin Solid Films 38 (1976) 143.
25. L. R. Zheng, L. S. Hung, J. W. Mayer, G. Majni, G. Ottaviani. Appl. Phys. Lett. 41 (1982) 646.
26. J. C. Ciccariello, S. Poize, P. Gas. J. Appl. Phys. 67 (1990) 3315.